Optimizing Urethral Healing with Anti-Inflammatory Nanofibers

Joceline S. Fuchs, MD **Arun K. Sharma, PhD**

Chicago, Illinois

Male urethral stricture disease occurs in approximately 2 to 12 of 1,000 men and has a substantial impact on quality of life and health care costs.[1] Urethroplasty is the gold standard treatment for stricture disease, with incorporation of graft when excision and primary anastomosis is not possible in cases of longer strictures.[2]

Although buccal mucosa is the most commonly used graft, with success rates ranging from 80% to 90%, pain and morbidity with harvest and donor site availability for extensive or recurrent strictures remain limitations.[3] Patients with underlying local tissue compromise, including previous urethral surgery, pelvic radiation, lichen sclerosus and hypospadias, pose a challenge with a higher risk of recurrent stricture.[4]

Two main goals in reconstructive urology are 1) finding alternative sources of graft material and 2) optimizing their long-term success. A key component of success involves modulation of the postoperative inflammatory process. While an inflammatory response following surgical tissue injury is essential for proper healing, dysfunctional or repetitive inflammatory responses can lead to poor tissue regeneration, fibrosis and surgical failure.

Protracted inflammation can result in pathological wound healing and scar formation, best illustrated in lichen sclerosus, a condition characterized by chronic inflammation resulting in progressive and recurrent urethral strictures.[5]

Despite advances in tissue engineering during the last several decades, engineered grafts remain limited by availability, variability and immunogenicity, as well as the cost and time required for autologous stem cell harvest and expansion. Reconstructive urologists continue to search for the "holy grail" of tissue engineering, meaning an affordable, unlimited, off-the-shelf graft or product that optimizes graft success. With this in mind, we investigated the targeted delivery of an anti-inflammatory molecule that has demonstrated promising effects in a rat bladder augmentation model.[6]

Peptide amphiphiles (PAs) are comprised of a hydrophobic alkyl segment attached to a peptide domain. These amphiphiles self-assemble in aqueous environments to produce a nanofiber and can be synthesized to present anti-inflammatory epitopes (AIF-PAs) at a density as high as 1×10^{14} epitopes per cm^2.[7] This allows for concentrated delivery of AIF-PAs in a gel form that outperforms any type of solid state delivery vehicle.

We investigated the use of AIF-PAs in a gel form applied to graft in a rat model of onlay urethroplasty.[8] We compared the outcomes of 36 Sprague Dawley® male rats undergoing ventral onlay urethroplasty using synthetic graft coated with AIF-PA1 (anti-inflammatory epitope), AIF-PA6 (control epitope) or left uncoated (control graft) (fig. 1). Tissue analysis was performed at 2, 12 and 25 days looking at 3 outcomes important in graft success, namely inflammation, fibrosis and urethral patency.

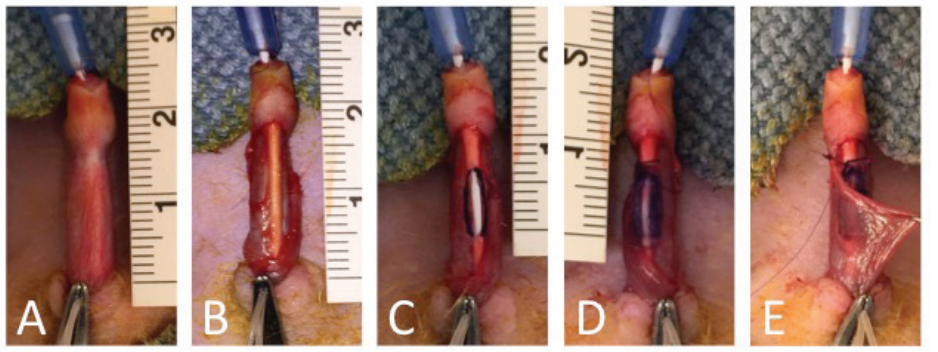

Figure 1. Description of graft urethroplasty in rat model. *A*, 22G venipuncture catheter is advanced into urethra. Tourniquet is applied at base of penis. *B*, circumcising incision is made, degloving penis. *C*, 6 mm ventral urethral incision is made. *D*, graft is sutured to cut urethral mucosal edges circumferentially with running 7-zero PDS®. *E*, circumcision incision is closed with 7-zero PDS.

AIF-PA1 positively altered the inflammatory landscape compared to the control AIF-PA6 and uncoated graft across multiple markers. AIF-PA1 treated urethras demonstrated modulation of the healing cascade, showing a 40% reduction in neutrophil markers (MPO) in the immediate postoperative period. This anti-inflammatory effect is mirrored by macrophage marker (CD68) reduction to less than half that of controls within the acute healing process. This is further supported by the nearly twofold up-regulation of postoperative anti-inflammatory marker interleukin-10.

Much of the literature regarding histological characterization of hypertrophic scars exists in the context of hypertrophic burn scars and keloids, with studies suggesting an increased ratio of collagen type III-to-collagen type I in hypertrophic or pathological scar formation compared to normal, mature scars and normal skin.[9] While collagen type III production by myofibroblasts is seen in the proliferative phase of wound healing, a shift toward rearrangement in an organized fashion with collagen type I is an indicator of wound maturation and remodeling with an increase in tensile strength.[10]

Subjects undergoing urethroplasty with AIF-PA1 treated graft demonstrated an accelerated transition to wound remodeling and scar maturation compared to controls. As highlighted in figure 2, a transition from collagen type III (in green) to collagen type I (in red) is seen by day 12 in AIF-PA1 subjects, while this shift is not seen until day 25 in the control groups.

Treatment of graft with AIF-PA1 triggered an initial 2.5-fold spike in periurethral collagen type III content, consistent with initial, robust collagen deposition, followed by a dramatic shift from collagen type III to type I, consistent with an early transition to tissue remodeling and maturation.

▼ Continued on page 18

Bacterial Strains and Chronic Pelvic Pain

▼ Continued from page 16

We imagine that such analysis of the host background and immune profile would reveal a "NOD-like" propensity toward CPPS in certain patients, mirroring the specificity seen in our mouse models. Furthermore, the data outlined go some way to explain the heterogeneity of CPPS in terms of the efficacy of antibiotics, as only in certain genetic contexts with certain bacterial strains do symptoms emerge. It is possible that the practical outcome of our study would lead to better screening of patients and their bacterial strains to determine responses to antibiotic therapy.

Awarded best poster at this year's AUA meeting in Boston, Massachusetts. ◆

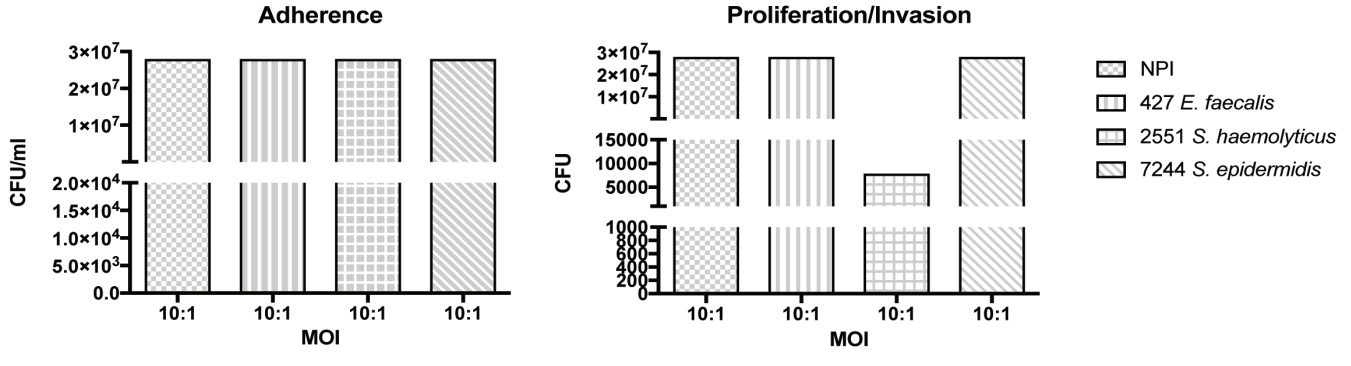

Figure 3. In vitro adherence and invasion assays for each gram-positive strain.

Tissue Engineering to Optimize Urethral Healing

▼ Continued from page 17

AIF-PA1 nanofibers promote accelerated wound healing in a rat graft urethroplasty model through faster resolution of perioperative inflammation and expedited transition to wound remodeling and maturation. While the efficacy of AIF-PAs remains limited to in vivo animal studies, it holds promise for future application in humans.

When attention to detail and precision are critical, and millimeters of stricture can mean the difference between success and failure, favorably altering the urethral healing microenvironment could have far-reaching implications for the future of reconstructive urology.

Awarded best poster at this year's AUA meeting in Boston, Massachusetts. ◆

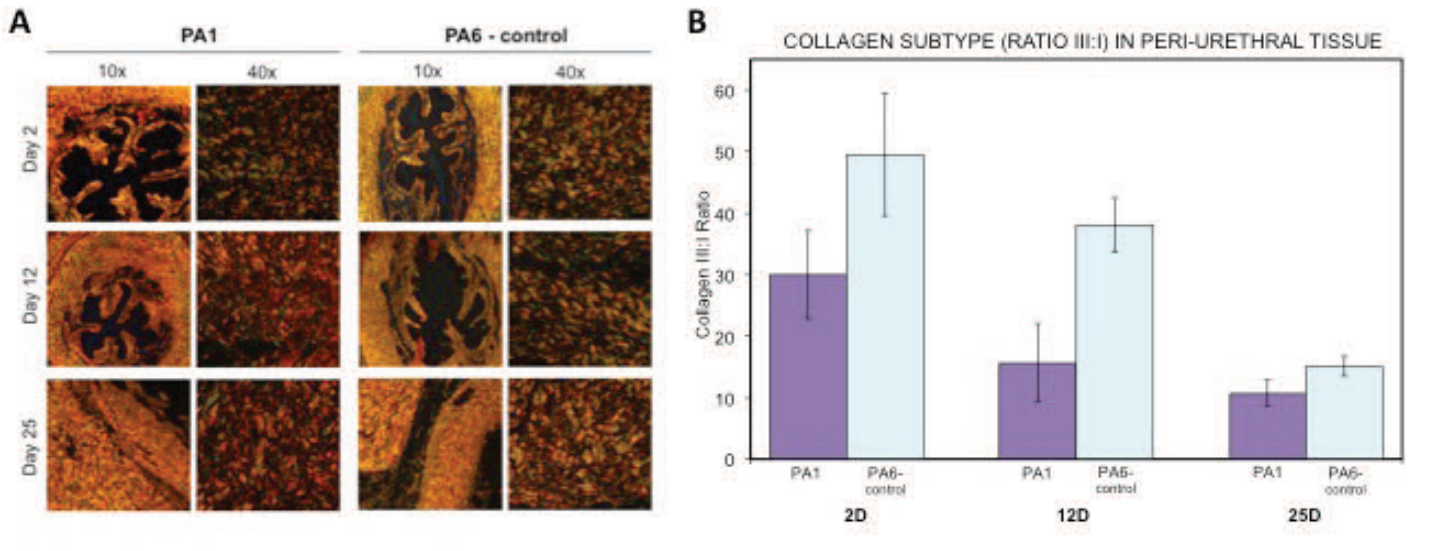

Figure 2. AIF-PA1 results in earlier transition to wound remodeling and maturation, and different proportion of collagen subtypes. *A*, polarized light photomicrographs of picrosirius staining demonstrates relative increase in collagen type III (green) in AIF-PA6 (control) over time, while AIF-PA1 animals transition to collagen type I (red yellow). *B*, AIF-PA1 treated animals demonstrate threefold reduction in collagen III:I ratio in AIF-PA1 group by day 12.

1. Santucci RA, Joyce GF and Wise M: Male urethral stricture disease. J Urol 2007; **177**: 1667.
2. Lumen N, Oosterlinck W and Hoebeke P: Urethral reconstruction using buccal mucosa or penile skin grafts: systematic review and meta-analysis. Urol Int 2012; **89**: 387.
3. Barbagli G, Kulkarni SB, Fossati N et al: Long-term followup and deterioration rate of anterior substitution urethroplasty. J Urol 2014; **192**: 808.
4. Breyer BN, McAninch JW, Whitson JM et al: Multivariate analysis of risk factors for long-term urethroplasty outcome. J Urol 2010; **183**: 613.
5. Pugliese JM, Morey AF and Peterson AC: Lichen sclerosus: review of the literature and current recommendations for management. J Urol 2007; **178**: 2268.
6. Bury MI, Fuller NJ, Meisner JW et al: The promotion of functional urinary bladder regeneration using anti-inflammatory nanofibers. Biomaterials 2014; **35**: 9311.
7. Silva GA, Czeisler C, Niece KL et al: Selective differentiation of neural progenitor cells by high-epitope density nanofibers. Science 2004; **303**: 1352.
8. Liu JS, Bury MI, Fuller NJ et al: Bone marrow stem/progenitor cells attenuate the inflammatory milieu following substitution urethroplasty. Sci Rep 2016; **6**: 35638.
9. Di Cesare PE, Cheung DT, Perelman N et al: Alteration of collagen composition and cross-linking in keloid tissues. Matrix 1990; **10**: 172.
10. Li J, Chen J and Kirsner R: Pathophysiology of acute wound healing. Clin Dermatol 2007; **25**: 9.

Novel Imaging and Urodynamics for Assessing Lower Urinary Tract Symptoms in Patients with Multiple Sclerosis

Jessica Eastman **Gary Lemack, MD**

Dallas, Texas

As many as 97% of patients with multiple sclerosis (MS) may experience lower urinary tract symptoms (LUTS) at some point after diagnosis, with approximately 10% experiencing detrusor or sphincter disorders before or at the time of diagnosis.[1] While the development of LUTS in this patient population may seem inevitable, the type and severity of the symptoms are greatly variable, and the presence or absence of symptoms does not reliably indicate the extent of lower urinary tract (LUT) dysfunction.[2]

Magnetic resonance imaging (MRI) is the cornerstone of the diagnosis and surveillance of patients with MS. Advances in magnetic resonance (MR) technology have revolutionized accurate disease staging and provide a framework for a logical and systematic approach to disease management. Still, remarkably little is known about the precise relationship between central nervous system (CNS) lesions and resultant LUT dysfunction. This study was undertaken to assess the relationship between CNS disease burden, LUTS and urodynamic findings using an innovative approach to objectively quantify disease burden and location.

An initial cohort of 30 patients was selected from a prospectively maintained institutional neurogenic bladder database. Each patient underwent a complete urodynamic study (UDS) within 1 year of the brain MRI being evaluated. Routine clinical MR images (T2-weighted fluid attenuated inversion recovery [FLAIR]) were segmented by a neuroradiologist blinded to clinical and UDS findings using a level tracing supervised semi-automated tool (3D Slicer),[3] with generation of masks containing an overall count (OC) of abnormal appearing voxels (fig. 1, *A* and *B*).

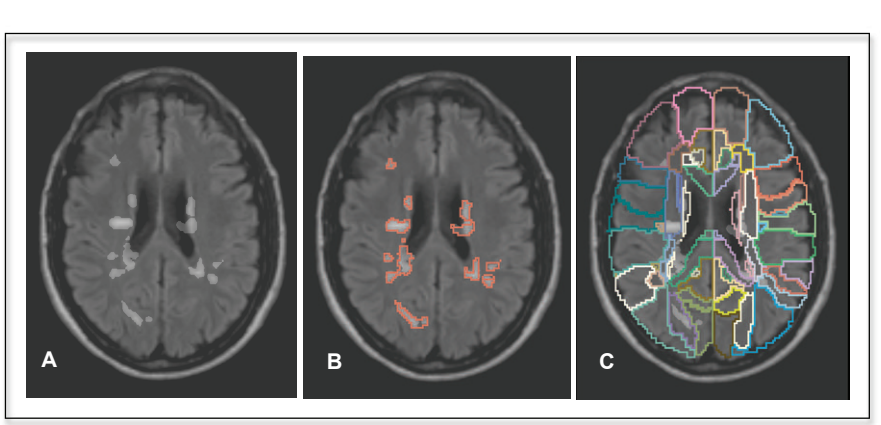

Figure 1. *A*, MS lesions are identified on MRI-FLAIR. *B*, OC and VDB in voxels are determined by level tracing semi-automated tool on segmented MRI. *C*, each MRI scan is normalized and superimposed to publicly available gray and white matter parcellation map to determine each brain lesion location.

Volume of disease burden (VDB, in cm^3) was obtained by multiplying OC by voxel dimensions (mm^3). The lesion masks and clinical images were then co-registered and normalized to a publicly available white and gray matter parcellation map to generate site specific disease volume measurements for each patient (fig. 1, *C*).[4] An additional subanalysis was completed on a subset of patients in this cohort who were identified as having had a cervical spine MRI within the same 1-year time frame.

We found no apparent correlation between lesion volume in the brain and either the UDS or quality of life (QOL) findings. This is consistent with other studies,[5] and supports our belief that lesion location has a much larger impact than overall lesion volume on LUT dysfunction in patients with MS.

We identified 12 out of 176 brain

▼ Continued on page 19